ACS Catalysis

Research Article

pubs.acs.org/acscatalysis

Recombinant Lipase Engineered with Amphipathic and Coiled-Coil Peptides

Kyung Seok Yang,[†,⊥] Bong Hyun Sung,[‡,⊥] Myung Keun Park,[†] Jun Hyoung Lee,[†] Ki Jung Lim,[†] Sung Chul Park,[†] Soo Jin Kim,[§] Hyung Kwoun Kim,[∥] Jung-Hoon Sohn,[‡] Ho Min Kim,*[,§] and Sun Chang Kim*[,†]

[†]Department of Biological Sciences, Korea Advanced Institute of Science and Technology, Daejeon 305-701, Korea

[‡]Bioenergy and Biochemical Research Center, Korea Research Institute of Bioscience and Biotechnology, Daejeon 305-806, Korea

[§]Graduate School of Medical Sciences and Engineering, Korea Advanced Institute of Science and Technology, Daejeon 305-701, Korea

[∥]Department of Biotechnology, Catholic University of Korea, Bucheon 420-743, Korea

Supporting Information

ABSTRACT: Lipases have been utilized industrially to produce biodiesel, oleochemicals, and pharmaceuticals. Many efforts such as metagenomics, directed evolution, and enzyme immobilization have been devoted to enhance the lipase activity. Here, we designed a recombinant lipase, NKC-M37-MAT, that was generated by incorporating an N-terminal amphipathic peptide (NKC) and a C-terminal coiled-coil peptide (MAT) into *Photobacterium lipolyticum* M37 lipase. The hydrophobic face of NKC improve the accessibility (K_m), and catalytic efficiency (K_{cat}/K_m) of the soluble lipase toward the hydrophobic substrate and tetrameric MAT further enhanced lipase catalytic activity (U/mg) through cooperative binding to its substrate such that the catalytic activity (U/mg) of NKC-M37-MAT was increased by a maximum of 54-fold compared with the wild-type, which decreased the biodiesel production time 5-fold from 30 to 6 h. This novel approach shows promise as a platform technology to increase lipase catalytic efficiency for industrial-scale production of biodiesel and biochemicals synthesized from hydrophobic substrates.

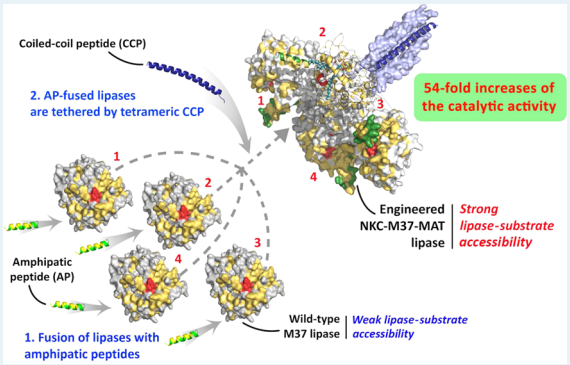

KEYWORDS: *lipase, catalytic activity, accessibility, amphipathic peptide, coiled-coil peptide, enzyme engineering, biocatalysis, biodiesel*

Triacylglycerol lipase (E.C. 3.1.1.3),[1] which catalyzes the hydrolysis of triglycerides to fatty acids and glycerols, plays an important role in industries that produce products such as detergents, food, leather, paper, cosmetics, and bioenergy.[1−3] Because of their broad substrate specificity and enantioselectivity, lipases have been utilized by the pharmaceutical industry to synthesize pure *R*- and *S*-optical isomers.[4] The energy industry is also using lipases to produce biodiesel from vegetable oil as well.[1,3,5,6]

Biodiesel products, an emerging renewable energy source, are produced through trans-esterification in the presence of a catalyst which could be basic (generally, NaOH), acid (usually, HCl or H_2SO_4), or enzymatic.[7−9] However, base-catalyzed trans-esterification is not feasible because alkaline can react with free fatty acid to form unwanted soap and water, which would affect the biodiesel quality and require extra investment for downstream separation and purification. In acid-catalyzed esterification, a large excess amount of alcohol is required in order to reach high biodiesel yield, and if sulfuric acid is utilized as the catalyst, it is difficult to remove after the reaction. Moreover, chemical-catalyzed trans-esterification produces toxic wastewater and consumes high amounts of energy to maintain high reaction temperature.[8] To overcome these problems, enzymatic methods using lipase are receiving special attention as an attractive alternative approach for biodiesel production. The great advantages of lipases compared with chemical catalysts are as follows: (1) relatively low reaction temperatures (approximately 40 °C),[6] (2) fewer process steps that generate reduced amounts of hazardous materials, and (3) improved product separation that generates higher purity glycerol.[5,6]

Because the enzymatic synthesis of biodiesel occurs at the lipid−water interface, increasing the accessibility of water-soluble lipase such as M37 to hydrophobic substrates is one of the most important but challenging factors required to improve the efficiency of enzymatic biodiesel production. Although surfactants are often used to solve this problem, other difficulties are encountered in separating surfactants from the

Received: December 23, 2014
Revised: July 14, 2015
Published: July 17, 2015

DOI: 10.1021/cs502079g
ACS Catal. 2015, 5, 5016−5025

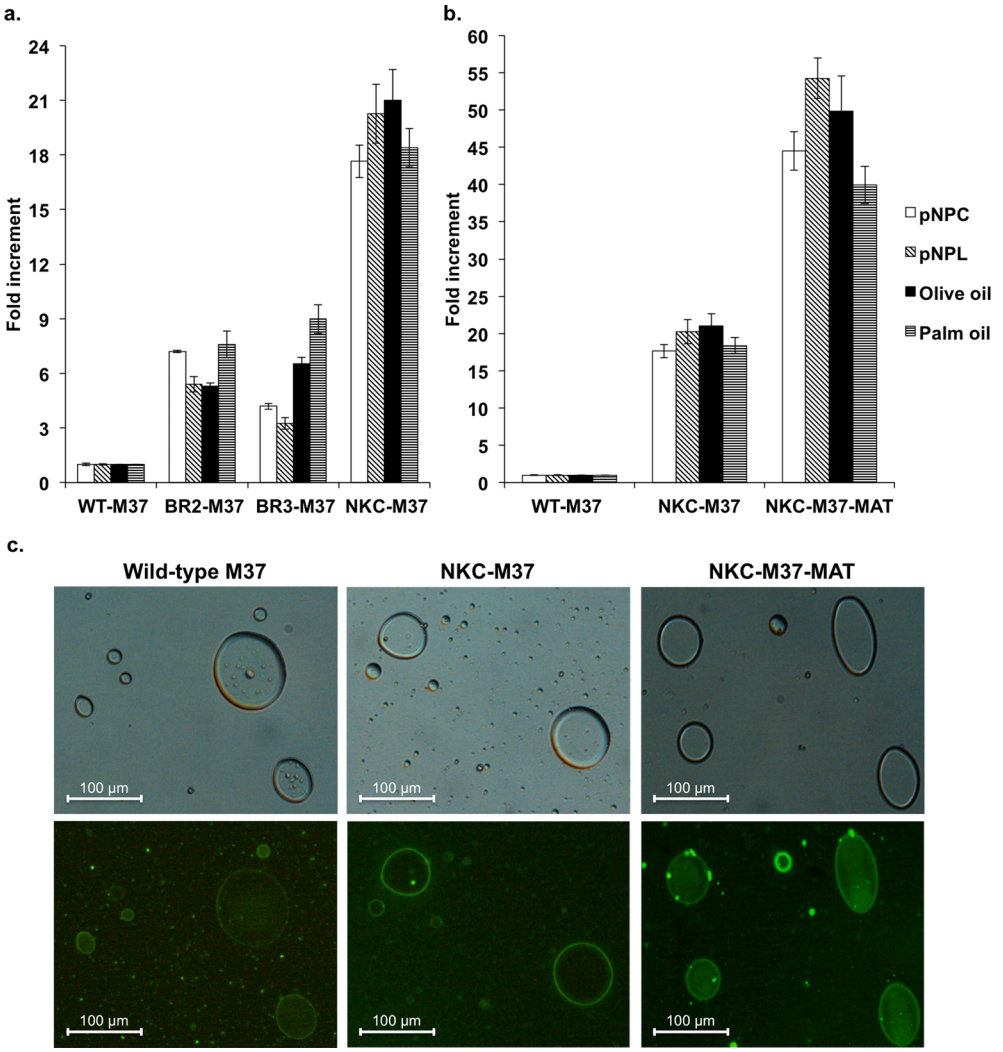

Figure 1. Characterization of wild-type, AP-fused M37, and oligomeric AP-fused M37 lipases. The effects of APs (a) and oligomerization (b) on the catalytic activity of the M37 lipase with various substrates (*p*NPC, *p*NPL, olive oil, and palm oil). (c) The localization of the AP-fused M37 lipase and its oligomeric complexes to lipid particles was determined using fluorescence microscopy. Wild-type M37 (left), NKC-M37 (middle), and tetrameric NKC-M37-MAT lipases (right). Upper row represents the bright-field image and lower row represents the fluorescence microscope image at 488 nm. Scale bars are shown in the diagram (100 μm). The number of fold increment was based on the catalytic activity of wild-type M37. The data represent the mean value of three independent experiments.

final reaction products as well as deactivation of the lipase by surfactants.[10,11] Techniques to enhance the activity, substrate-specificity, thermal resistance, and methanol tolerance of lipases include approaches such as metagenomics,[12,13] directed evolution,[14,15] structure-based protein engineering,[16,17] and enzyme immobilization.[18−20] However, a fundamental solution that improves substrate accessibility remains elusive.[10,11] Therefore, engineering the lipases to improve the accessibility may be an appropriate way to increase efficiency of the biodiesel synthesis in combination with the engineering of lipases to improve K_{cat}.

Here, in order to enhance the substrate accessibility of lipase, we designed a recombinant lipase, which contains an amphipathic peptide (AP) and a coiled-coil peptide (CCP) at its N-terminal and C-terminal, respectively. We first investigated the effect of AP on lipase activity. The AP is a continuous α-helical peptide with hydrophilic and hydrophobic amino acid residues on the two opposite faces, respectively. Thus, the hydrophobic face interacts preferentially with long fatty-acyl chains of the lipid substrate, triacylglycerol. The catalytic activity (U/mg) of the AP-fused lipases for hydrophobic substrates (*p*NPC and *p*NPL) was increased by a maximum of 20-fold (Figure 1a and Table 1).

Next, we determined the effect of CCP on lipase activity. CCPs contain a structural motif comprising two to five intertwined α-helices that typically mediate oligomerization.[21] CCP-fused lipases form a bundle tethered by oligomeric CCPs; therefore, each lipase binds cooperatively to the substrate. The catalytic activity (U/mg) of the CCP-fused AP-lipase was increased by a factor of approximately 3 in comparison to the monomer AP-lipase. The overall activities of the engineered lipases containing APs and CCPs were increased by factors of as much as 54 compared with wild-type lipase, which increased biodiesel production efficiency 5-fold. This engineered lipase may replace chemical catalysts as well as lipases currently used for biodiesel production. Moreover, the AP- and CCP-fusion approaches may serve as a platform technology to improve the catalytic activity of other enzymes with hydrophobic substrates.

DOI: 10.1021/cs502079g
ACS Catal. 2015, 5, 5016−5025

Table 1. Catalytic Activities of the AP-Fused Lipases and Their Tetrameric Complexes with Various Substrates

lipase	catalytic activity (U/mg)[a]							
	*p*NPC	relative activity[b]	*p*NPL	relative activity[b]	olive oil	relative activity[b]	palm oil	relative activity[b]
wild-type M37	$3.43 \times 10^1 \pm 0.17 \times 10^1$	1	$6.42 \times 10^1 \pm 0.32 \times 10^1$	1	$1.58 \times 10^2 \pm 0.18 \times 10^2$	1	$1.93 \times 10^2 \pm 0.19 \times 10^2$	1
BR2-M37	$2.47 \times 10^2 \pm 0.20 \times 10^2$	7	$3.47 \times 10^2 \pm 0.28 \times 10^2$	5	$8.35 \times 10^2 \pm 0.70 \times 10^2$	5	$1.44 \times 10^3 \pm 0.41 \times 10^2$	7
BR3-M37	$1.43 \times 10^2 \pm 0.14 \times 10^2$	4	$2.09 \times 10^2 \pm 0.21 \times 10^2$	3	$1.02 \times 10^3 \pm 0.62 \times 10^2$	6	$1.71 \times 10^3 \pm 0.20 \times 10^2$	9
NKC-M37	$6.06 \times 10^2 \pm 0.48 \times 10^2$	18	$1.30 \times 10^3 \pm 0.10 \times 10^3$	20	$3.26 \times 10^3 \pm 0.11 \times 10^3$	21	$3.52 \times 10^3 \pm 0.15 \times 10^3$	18
NKC-M37-MAT	$1.53 \times 10^3 \pm 0.15 \times 10^3$	45	$3.49 \times 10^3 \pm 0.17 \times 10^3$	54	$7.72 \times 10^3 \pm 0.15 \times 10^3$	49	$7.63 \times 10^3 \pm 0.29 \times 10^3$	40
wild-type L1	$2.89 \times 10^1 \pm 0.06 \times 10^1$	1	$3.33 \times 10^1 \pm 0.07 \times 10^1$	1	$1.34 \times 10^2 \pm 0.15 \times 10^2$	1	$1.64 \times 10^2 \pm 0.19 \times 10^2$	1
BR2-L1	$1.22 \times 10^2 \pm 0.61 \times 10^1$	4	$1.40 \times 10^2 \pm 0.11 \times 10^2$	4	$2.83 \times 10^2 \pm 0.38 \times 10^2$	2	$3.17 \times 10^2 \pm 0.38 \times 10^2$	2
BR3-L1	$1.29 \times 10^2 \pm 0.65 \times 10^1$	4	$1.49 \times 10^2 \pm 0.12 \times 10^2$	4	$3.40 \times 10^2 \pm 0.42 \times 10^2$	3	$3.67 \times 10^2 \pm 0.43 \times 10^2$	2
NKC-L1	$1.88 \times 10^2 \pm 0.24 \times 10^2$	6	$3.48 \times 10^2 \pm 0.45 \times 10^2$	10	$1.01 \times 10^3 \pm 0.35 \times 10^2$	8	$1.09 \times 10^3 \pm 0.37 \times 10^2$	7
NKC-L1-MAT	$4.27 \times 10^2 \pm 0.64 \times 10^2$	15	$8.12 \times 10^2 \pm 0.12 \times 10^3$	24	$2.72 \times 10^3 \pm 0.52 \times 10^2$	20	$2.69 \times 10^3 \pm 0.51 \times 10^2$	16
wild-type TliA	$2.69 \times 10^1 \pm 0.08 \times 10^1$	1	$5.04 \times 10^1 \pm 0.15 \times 10^1$	1	$1.27 \times 10^2 \pm 0.15 \times 10^2$	1	$1.55 \times 10^2 \pm 0.18 \times 10^2$	1
BR2-TliA	$8.16 \times 10^1 \pm 0.41 \times 10^1$	3	$1.11 \times 10^2 \pm 0.89 \times 10^1$	2	$1.88 \times 10^2 \pm 0.21 \times 10^2$	1	$2.04 \times 10^2 \pm 0.27 \times 10^2$	1
BR3-TliA	$8.81 \times 10^1 \pm 0.44 \times 10^1$	3	$1.18 \times 10^2 \pm 0.94 \times 10^1$	2	$2.14 \times 10^2 \pm 0.30 \times 10^2$	2	$2.31 \times 10^2 \pm 0.31 \times 10^2$	2
NKC-TliA	$1.48 \times 10^2 \pm 0.25 \times 10^2$	6	$3.12 \times 10^2 \pm 0.53 \times 10^2$	6	$8.00 \times 10^2 \pm 0.27 \times 10^2$	6	$8.62 \times 10^2 \pm 0.29 \times 10^2$	6
NKC-TliA-MAT	$3.11 \times 10^2 \pm 0.56 \times 10^2$	12	$6.86 \times 10^2 \pm 0.12 \times 10^3$	14	$1.81 \times 10^3 \pm 0.35 \times 10^2$	14	$1.79 \times 10^3 \pm 0.34 \times 10^2$	12

[a]The data shown are the mean and standard deviation for three independent experiments. [b]Relative activity = [U/mg (engineered)]/[U/mg (wild-type)].

RESULTS

Engineering Lipases with AP and CCP Domains. To increase the accessibility of a lipase to its hydrophobic substrate, a super lipase was constructed by incorporating N-terminal AP and C-terminal CCP sequences. The general scheme of our AP-lipase-CCP fusion system is depicted in Figure 2, and the amino acid sequences of the APs used in this study and the amphipathic α-helical structure shown as an α-helical wheel projection are presented in Figure S1. The APs BR2, BR3, and NKC were fused to three different lipases (M37,[22] L1,[23] and TliA[24]), respectively, via a flexible G_4S linker, to construct the lipases designated BR2-M37, BR3-M37, NKC-M37, BR2-L1, BR3-L1, NKC-L1, BR2-TliA, BR3-TliA, and NKC-TliA. To further increase enzymatic activity by enhancing cooperative interactions between lipase molecules, short CCPs such as GCN4,[25] MAT,[21,26,27] and COMP[28] were incorporated into the NKC-M37 lipase, which showed the highest enzyme catalytic activity, to generate dimeric (NKC-M37-GCN4), tetrameric (NKC-M37-MAT), and pentameric (NKC-M37-COMP) lipases. We chose the NKC-M37-MAT lipase fusion for further study, as it showed the highest enzymatic activity (Figure S2). After Ni-affinity purification and ion exchange chromatography, the majority (~70%) of NKC-M37-MAT were tetramers. The molecular masses of monomeric wild-type M37 and tetrameric NKC-M37-MAT lipases, which were determined using gel filtration, were 41 kDa and 164 kDa, respectively (Figure 3). Transmission electron microscopy analysis shows that the NKC-M37-MAT lipase formed tetramers tethered through the MAT peptide, and the wild-type M37 lipase formed monomers (Figure 3).

Catalytic Activity of Engineered Lipases. The catalytic activity (U/mg) of the wild-type M37 lipase with the substrate *p*-nitrophenyl laurate (*p*NPL) was 64.24 U/mg. Lipase activity increased by a factor of approximately 5, 3, or 20 when the AP BR2, BR3, or NKC, respectively, was incorporated (Figure 1a and Table 1). The activity of NKC-M37 was the highest (1300.86 U/mg). Using olive oil as the substrate, the catalytic activity of NKC-M37 was 3264.05 U/mg, which was higher by a factor of approximately 21 compared with that of the wild-type M37 lipase. The results obtained using palm oil were similar (Figure 1a and Table 1). To determine whether this approach was generally applicable, we incorporated BR2, BR3, and NKC into the L1 and TliA lipases. Same as the former case of M37 lipase, the catalytic activities of the NKC-L1 and NKC-TliA lipases presented the most increment in activity compared to other types of AP-fused lipases, and their catalytic activities (U/mg) were higher by factors of approximately 10 and 6, respectively, compared with those of wild-type (Table 1).

The catalytic activity (U/mg) of the CCP-fused M37 lipases without AP increased by only 20% to 60% compared to the wild-type M37 lipase, and the tetrameric M37-MAT lipase showed the greatest increase in activity of all the oligomeric M37 lipases (Figure S3). The catalytic activity (U/mg) of the NKC-M37-MAT lipase increased about 300% versus the NKC-M37 lipase (Figure S2). Further, the catalytic activities of the tetrameric NKC-L1-MAT and NKC-TliA-MAT lipases were higher by factors of 2.3 and 2.2 compared with those of the

DOI: 10.1021/cs502079g
ACS Catal. 2015, 5, 5016−5025

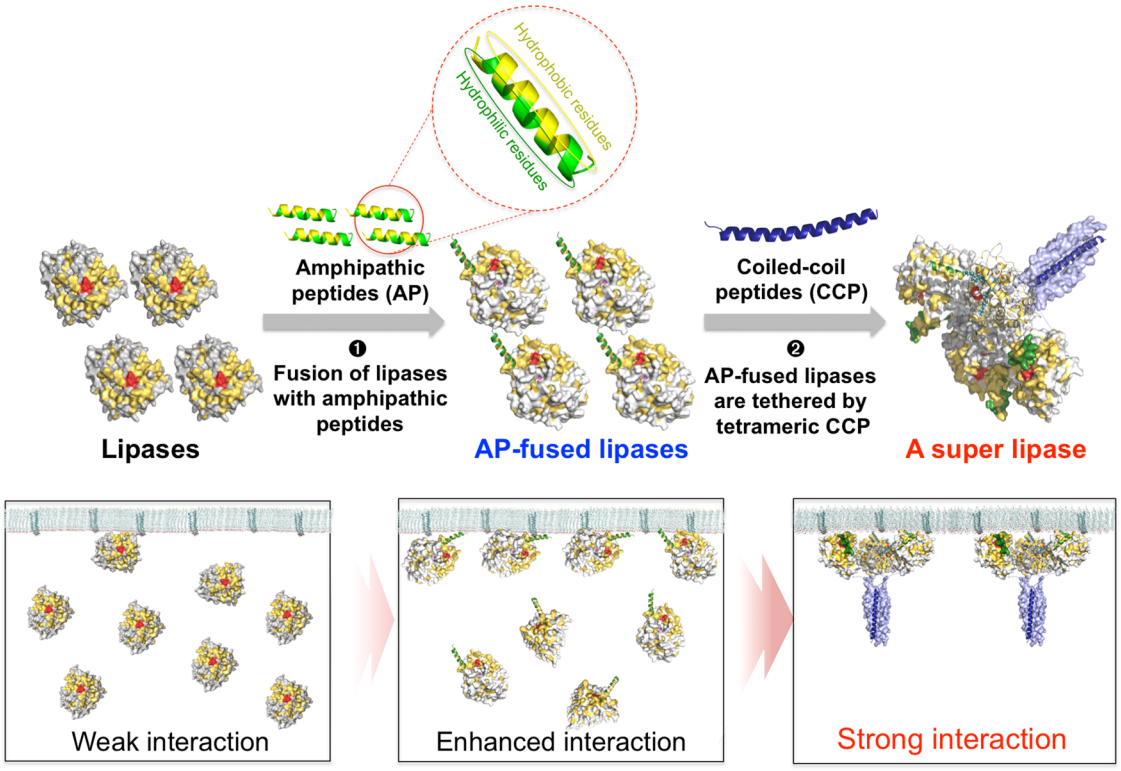

Figure 2. General scheme of the amphipathic peptide-fused lipase and oligomerization. Recombinant lipases were generated with an amphipathic peptide and then tethered with a coiled-coil peptide to induce the formation of tetrameric lipases. The structure of M37 lipase is taken from PDB (PDB ID: 2ORY). The structures of NKC and MAT were modeled using the I-TASSER server. Hydrophobic residues are yellow and the lid helix including the active site is red. The hydrophobic region of NKC is yellow, the hydrophilic region is green, and MAT is blue.

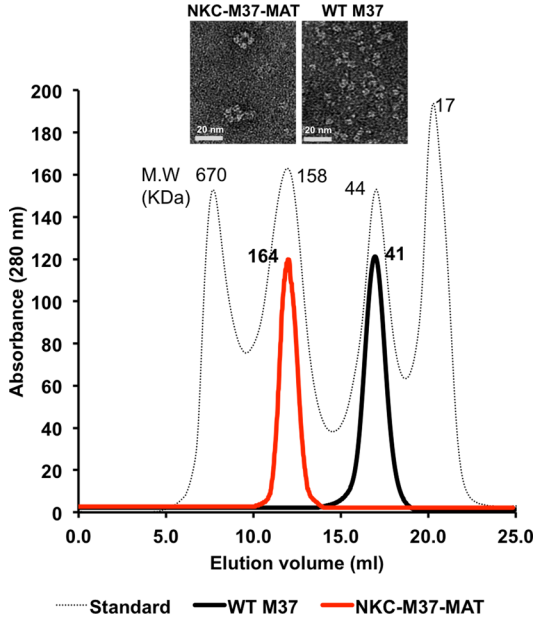

Figure 3. Gel filtration elution profiles of the tetrameric NKC-fused M37 lipase. Dotted black, red, and solid black lines represent standards, tetrameric NKC-M37-MAT, and monomeric wild-type M37 lipases, respectively. The molecular weights of the lipases were estimated from the molecular weight of standard markers. Molecular weights of standard markers are shown above each peak. Upper images are transmission electron microscopy analysis of wild-type M37 (upper right; scale bar = 20 nm) and tetrameric NKC-M37-MAT lipases (upper left; scale bar = 20 nm).

monomeric, NKC-fused versions, respectively (Table 1). Overall, the catalytic activity (U/mg) of the tetrameric NKC-M37-MAT lipase was higher by a factor of approximately 54 compared with that of the wild-type M37 lipase (Figure 1b).

The enzymatic kinetic parameters of the lipases are analyzed in Table 2 and Figure S4. The catalytic efficiency (K_{cat}/K_m) of the NKC-M37 lipase was higher by a factor of approximately 19 than that of the wild-type M37 lipase. We attribute these findings to the higher accessibility between the enzyme and its substrate (K_m). The results for the NKC-M37 lipase were the most significant, because its K_m value was lower by a factor of approximately 7, and its K_{cat} value was higher by a factor of approximately 3 compared with those of the wild-type M37 lipase. The K_{cat}/K_m values of the NKC-L1 and NKC-TliA lipases were significantly increased by factors of approximately 10 and 6, respectively, compared with those of the wild-type lipases (Table 2).

The catalytic efficiency (K_{cat}/K_m) of the tetrameric NKC-M37-MAT lipase was the highest. Thus, the K_m and K_{cat} values of the tetrameric NKC-M37-MAT lipase were lower by a factor of 2 and slightly higher, respectively, compared with those of the monomeric NKC-M37 lipase (Table 2). The K_m values of the NKC-L1-MAT and NKC-TliA-MAT lipases were lower by factors of 2.3 and 1.6, respectively, compared with those of their monomeric counterparts, whereas their K_{cat} values were slightly increased.

The monomeric lipases were tethered through their CCP domains, and they bound to their lipid substrates in a cooperative manner. TEM analysis and gel-filtration analysis clearly demonstrated that the purified NKC-M37-MAT form tetramers. To determine the cooperative activity of each NKC-

DOI: 10.1021/cs502079g
ACS Catal. 2015, 5, 5016−5025

Table 2. Kinetic Parameters of the Engineered Lipases Used in This Study[a]

lipase	K_m (mM)	K_{cat} (min^{-1})	K_{cat}/K_m (sec^{-1} M^{-1})	relative specificity[b]
wild-type M37	$0.57 \times 10^{0} \pm 0.52 \times 10^{-1}$	$3.64 \times 10^{2} \pm 0.12 \times 10^{2}$	1.07×10^{4}	1.0
BR2-M37	$0.18 \times 10^{0} \pm 0.13 \times 10^{-1}$	$5.44 \times 10^{2} \pm 0.28 \times 10^{2}$	4.98×10^{4}	4.7
BR3-M37	$0.25 \times 10^{0} \pm 0.18 \times 10^{-1}$	$5.24 \times 10^{2} \pm 0.21 \times 10^{2}$	3.52×10^{4}	3.3
NKC-M37	$0.82 \times 10^{-1} \pm 0.40 \times 10^{-2}$	$1.01 \times 10^{3} \pm 0.41 \times 10^{2}$	2.05×10^{5}	19.2
M37-GCN4	$0.45 \times 10^{0} \pm 0.38 \times 10^{-1}$	$3.60 \times 10^{2} \pm 0.15 \times 10^{2}$	1.34×10^{4}	1.3
M37-MAT	$0.37 \times 10^{0} \pm 0.24 \times 10^{-1}$	$3.60 \times 10^{2} \pm 0.11 \times 10^{2}$	1.64×10^{4}	1.5
M37-COMP	$0.50 \times 10^{0} \pm 0.64 \times 10^{-1}$	$3.62 \times 10^{2} \pm 0.14 \times 10^{2}$	1.20×10^{4}	1.1
NKC-M37-MAT	$0.41 \times 10^{-1} \pm 0.30 \times 10^{-2}$	$1.05 \times 10^{3} \pm 0.55 \times 10^{2}$	4.25×10^{5}	39.7
wild -type L1	$0.65 \times 10^{0} \pm 0.48 \times 10^{-1}$	$2.91 \times 10^{2} \pm 0.13 \times 10^{2}$	7.49×10^{3}	1.0
NKC-L1	$0.17 \times 10^{0} \pm 0.12 \times 10^{-1}$	$7.19 \times 10^{2} \pm 0.34 \times 10^{2}$	7.26×10^{4}	9.7
NKC-L1-MAT	$0.72 \times 10^{-1} \pm 0.80 \times 10^{-2}$	$7.20 \times 10^{2} \pm 0.38 \times 10^{2}$	1.67×10^{5}	22.3
wild-type TliA	$0.62 \times 10^{0} \pm 0.41 \times 10^{-1}$	$3.03 \times 10^{2} \pm 0.13 \times 10^{2}$	8.14×10^{3}	1.0
NKC-TliA	$0.25 \times 10^{0} \pm 0.16 \times 10^{-1}$	$6.72 \times 10^{2} \pm 0.29 \times 10^{2}$	4.52×10^{4}	5.6
NKC-TliA-MAT	$0.15 \times 10^{0} \pm 0.40 \times 10^{-2}$	$6.84 \times 10^{2} \pm 0.37 \times 10^{2}$	7.50×10^{4}	9.2
CalB[38]	$0.41 \times 10^{0} \pm 0.40 \times 10^{-1}$	$3.05 \times 10^{2} \pm 0.10 \times 10^{2}$	1.24×10^{4}	

The rates of hydrolysis of *p*NPL by the wild-type and engineered lipases were determined in 150 μL reaction volumes containing 10 μg of lipase at 40 °C. The production of *p*-nitrophenolate was measured at 405 nm. All experiments were repeated three times. Kinetic constants were calculated by fitting the initial rates to the Michaelis–Menten equation. [a]The data shown are the mean and standard deviation for three independent experiments. [b]Relative specificity = $[K_{cat}/K_m$ (engineered)$]/[K_{cat}/K_m$ (wild-type)$]$

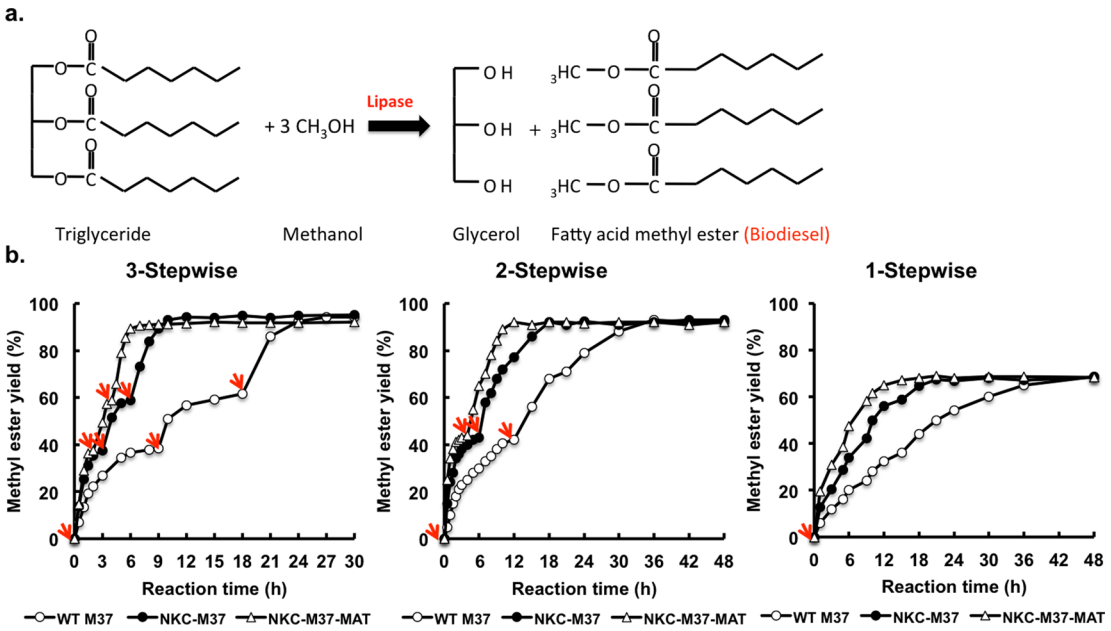

Figure 4. Analysis of the methanol resistance of the NKC-M37 lipases and tetrameric NKC-M37-MAT lipase and their application to biodiesel production. (a) Overview of biodiesel production from triglycerides catalyzed by lipase. In the transesterification reaction, triglycerides react with an alcohol, typically methanol, to produce biodiesel (fatty acid methyl ester) and glycerol. (b) Biodiesel production from olive oil using the wild-type M37, NKC-M37, and tetrameric NKC-M37-MAT lipases. The amounts of biodiesel produced were measured quantitatively using GC. The quantities (in moles) of biodiesel in the reaction mixtures were calculated by comparing the retention times and peak areas of standard fatty acid methyl ester peaks. Time course of the three-step transesterification of olive oil using the wild-type M37, NKC-M37, and tetrameric NKC-M37-MAT lipases (left). Time course of two-step (middle) and one-step (right) transesterification of olive oil using the wild-type and engineered lipases, respectively. The red arrows indicate the addition of methanol to the reaction mixture.

M37-MAT in this tetrameric form, the Hill coefficient was calculated on the basis of a numerical fit to the reaction velocity (Figure S5).[29] The Hill coefficient of the tetrameric NKC-M37-MAT lipase was 2.1 ± 0.2, which indicates that activities of the lipase molecules were cooperatively coupled.

Fluorescence Microscopy Analysis of the Interaction between a Lipase and Its Substrate. To address the effects of AP and CCP sequences on the accessibility of a lipase to its substrate, the localizations of the wild-type M37, NKC-M37, and NKC-M37-MAT lipases relative to lipid particles were determined using fluorescence microscopy (Figure 1c and Figure S6). This analysis revealed that the majority of NKC-M37 molecules localized to the surface of oil droplets. In contrast, the majority of the wild-type M37 molecules were not closely associated with the lipid particles and were instead dispersed throughout the solution. In comparison, the association between the tetrameric NKC-M37-MAT lipase and lipid particles was the highest.

Thermal Stability and Methanol Tolerance of Engineered Lipases. The residual activities of the wild-type M37

DOI: 10.1021/cs502079g
ACS Catal. 2015, 5, 5016–5025

lipase and NKC-M37 lipase were 76% at 40 °C; they decreased significantly to 57% at 45 °C and then to 5% at 70 °C after 30 min. However, the tetrameric NKC-M37-MAT lipase maintained 73% of its activity at 45 °C (Figure S7a). Further, the thermal denaturation of the wild-type M37 and tetrameric NKC-M37-MAT lipases was monitored by measuring ellipticity at 193 nm when they were heated at 10 °C/min from 20 to 70 °C. Ellipticity decreased as the temperature increased, consistent with the denaturation of protein secondary structure (Table S1).[30] Indeed, the ellipticity of the tetrameric NKC-M37-MAT lipase changed much more slowly during the temperature ramp compared with the wild-type M37 (Figure S7b and c). Circular dichroism analysis showed that the increased stability was conferred exclusively by the tetrameric form of the lipase, as monomers have a T_m of 43 °C, while tetramers show an increase of 8 °C. The high thermal stability of the tetrameric NKC-L1-MAT lipase was similar to L1 lipase (Figure S7d, e, and f).

The NKC-M37 and NKC-M37-MAT lipases exhibited the methanol tolerance similar to the wild-type M37 lipase in 3.3%, 5%, and 10% methanol solution at 40 °C for 12 h (Figure S8)

Biodiesel Production Using Engineered Lipases. We next analyzed the conversion of olive and palm oils into biodiesel by the NKC-M37 and tetrameric NKC-M37-MAT lipases (Figure 4a). When three-step methanol addition was performed, TLC analysis showed that the wild-type M37 and NKC-M37-MAT lipases converted most of the olive oil to biodiesel (Figure S9), and GC analysis showed that the wild-type M37 and NKC-M37 lipases converted 95% of the olive oil into biodiesel after 30 and 10 h, respectively. Further, the tetrameric NKC-M37-MAT lipase required only 6 h to reach the same yield (Figure 4b). Using two-step methanol addition, the tetrameric NKC-M37-MAT lipase produced an amount of biodiesel in 12 h equal to that produced by the wild-type M37 lipase after 36 h (Figure 4b). Using one-step methanol addition, the respective times to reach the same yields were 12 and 48 h (Figure 4b). Similar results were obtained when palm oil and soybean oil waste were used as substrates (Figure S10).

DISCUSSION

In the present study, we generated a recombinant lipase by incorporating N-terminal AP and C-terminal CCP domains, and its catalytic activity (U/mg) was higher by a factor of approximately 54 compared with the wild-type enzyme. Lipolysis is catalyzed at the oil−water interface and is naturally very slow, because the initial binding of a lipase to its substrate is relatively weak. We reasoned that the AP domain should increase substrate-binding accessibility and that the CCP domain should mediate formation of enzyme oligomers to further increase lipase activity through cooperative binding to its substrate (Figure 2).

The increased enzymatic efficiency of the lipase (Figure 1 and Table 2) may be explained as follows: (i) a shift in lipase partitioning from the water phase to the lipid−water interface, an increase in the proximity and local concentration of enzymes around the lipid substrates, and maximizing of the reaction rate, as demonstrated by the catalytic efficiency (K_{cat}/K_m); and (ii) cooperative interaction between lipase and substrate as confirmed by the Hill coefficient of the engineered lipases.

The lipases are water-soluble, yet they must interact with hydrophobic substrates. APs are polar along one surface of their helices and hydrophobic on the other, providing a structural organization that allows them to interact with hydrophobic and hydrophilic environments (Figure S2). The characteristics of the linear APs and their interaction with lipid substrates resemble the properties of surfactants. Therefore, we reasoned that the incorporation of an AP domain might improve lipase-lipid interactions. Depending on amphipathicity, we found that introducing an AP domain increased catalytic activity by a factor as much as 20, a striking result obtained without modification of the active site. The recombinant lipase with the NKC sequence, which is more amphipathic than BR2 or BR3, showed the highest lipase activity (Figure 1a).

Although *Candida antarctica* lipase B (CalB) is widely used as a biodiesel production enzyme, we used M37 lipase in our experiment because the M37 lipase is more methanol-tolerant than CalB lipase in high concentration (∼10% v/v) of methanol.[22,31] This stability gives M37 lipase higher efficiency than other lipases in biodiesel production that consume a mass amount of methanol during the production process.

Protein conformation might help explain the positive effects of the NKC AP domain on the specific activity of the NKC-M37 lipase that hydrolyzed *p*NPL at a rate that was approximately higher by a factor of approximately 20 compared with that of the wild-type M37 lipase. We speculated that the AP domain might affect the conformation of the region surrounding the active site and the lid domain, which covers the active site. Lipases exist in equilibrium between a closed conformation, in which the active site is separated from the reaction medium by the lid, and an open conformation, in which the lid is displaced to fully expose the active site to the reaction medium.[32] Recently, Palomo et al. reported lipase variants with site-specific incorporation of rationally designed peptides into the lipase-lid site and showed that lipase activation involves large structural rearrangements and a more open conformation of the lid with the peptide modification.[33,34] The active site of M37 lipase is covered by an α helical lid (α3), and the conformation of the lid is strongly influenced by the helices α9 and α10.[35] The NKC was incorporated into the N-terminus of the M37 lipase near the α10 helix and might modify the mobility of the lid. Accordingly, NKC might improve the access of hydrophobic substrates to the active site and increase binding accessibility. Further, the helical lid of the M37 lipase is shorter compared with those of the L1 and TliA lipases, possibly explaining differences in the enhancing effect of the AP domain on catalytic activity.

The spatial organization of enzymes plays a crucial role in their functionality and efficiency.[36] The CCP domains may tether lipases to induce cooperative binding to its substrate and reduce the dissociation rate. Thus, when one lipase binds to a lipid substrate, subsequently it increases the binding efficiencies of the second and third enzyme molecules in the bundle complex, similar to the binding of oxygen to hemoglobin.[37] According to the Hill coefficient results, when the Hill coefficient is 1, it represents noncooperative binding that the affinity of the enzyme for a substrate is not dependent on. When the Hill coefficient is higher than 1, it represents positively cooperative binding that once one enzyme is bound to the substrate, its affinity for other enzymes is increased. In the case of tetrameric NKC-M37-MAT, the Hill coefficient is 2.1, which represents positively cooperative binding. Such a mechanism explains why the activities of the oligomeric lipases were higher compared with monomeric lipases. For example, the catalytic activities (U/mg) of the dimeric NKC-M37-GCN4 and tetrameric NKC-M37-MAT lipases were higher by factors of approximately 2 and 3 compared with that of the monomeric

DOI: 10.1021/cs502079g
ACS Catal. 2015, 5, 5016−5025

NKC-M37 lipase, respectively (and higher by factors of approximately 45 and 54 compared with that of the wild-type M37 lipase). However, the catalytic activity of the pentameric NKC-M37-COMP lipase was lower than that of the tetrameric NKC-M37-MAT lipase, possibly because of steric hindrance of a large multimer (Figure S2).[33] When CCP was fused with the lipases, enzymatic activity increased by only 20% to 60%; however, in the case of both AP and CCP fused lipases, enzymatic activity increased by 300% (Figure S3).

As shown by fluorescence microscopy analysis, the NKC-M37 lipase localized to lipid particles more frequently compared with the wild-type M37 (Figure 1c and Figure S6). This association was more pronounced for the tetrameric NKC-M37-MAT lipase. Thus, the presence of AP and CCP domains induced significant changes in the partitioning of the lipase between the water phase and the lipid−water interface. The K_m values of the NKC-M37 and NKC-M37-MAT lipases were lower by factors of approximately 7 and 14 compared with wild-type lipase, respectively, and the catalytic efficiency (K_{cat}/K_m) of the NKC-M37 and NKC-M37-MAT lipases were increased by factors of approximately 19 and 40 compared with the wild-type lipase, respectively (Table 2). Further, the catalytic efficiency (K_{cat}/K_m) of the tetrameric NKC-M37-MAT lipase was higher by a factor of approximately 35 compared with wild-type of *Candida antarctica* lipase B (CalB),[38] which is most widely used in the industry and indicates that the recombinant NKC-M37-MAT lipase is more suitable for industrial use. Furthermore, our novel approach introducing AP and CCP domains can also be applicable to the immobilized lipase for the multiple usage.

The thermal stability of the tetrameric NKC-M37-MAT lipase was higher compared with that of the monomeric wild type-M37 lipase, and the NKC-M37 and tetrameric NKC-M37-MAT lipases were also quite stable in methanol, similar to the wild-type M37 lipase, which is a property required for efficient biodiesel production (Figure S7 and Figure S8). The oligomerization of lipase induced by the CCP domain (MAT) might increase stability by decreasing structural flexibility, which may decrease unfolding and denaturation (Figure S7). Therefore, their stabilities at high temperature and in the presence of high concentrations of methanol suggest that our engineered lipases might have applications in many areas of industrial biochemical production that involve hydrophobic substrates and organic solvents.[39]

The NKC-M37-MAT lipase was applied to biodiesel production and increased biodiesel production efficiency 5-fold (Figure 4b). Although no linear relationship between a catalytic efficiency and transesterification efficiency was found, we speculate that the substrate for NKC-M37-MAT, which is ~80% of the entire reaction volume for biodiesel production, explains that the influence of increased accessibility to the substrate for biodiesel production by NKC may thus not be as high as that of the conditions for Michaelis−Menten kinetics with *p*NPL hydrolysis.

Cost-effective production of biodiesel requires minimizing the methanol treatment step. The NKC-M37-MAT lipase produced biodiesel very efficiently even using the one-step methanol treatment process, and the production time decreased by greater than 80% compared with the other industrial lipases, even when the two- and three-step methods were used.

Notably, the feedstock accounts for greater than 70% of biodiesel production cost.[40] Intensive research is underway on using low cost feedstocks such as waste cooking oil, beef tallow, pork lard, and yellow grease to make the cost of producing biodiesel competitive with that for petro-diesel.[40] The engineered NKC-M37-MAT lipase produced biodiesel very efficiently, even from waste cooking oil, which includes impurities, free fatty acids, and water, but at reduced yield compared with oils (Figure S10). Therefore, we conclude that engineering lipases with AP and CCP to improve accessibility may be an attractive way to improve the biodiesel synthesis efficiency in combination with the engineering of lipases to improve K_{cat}.

METHODS

Bacterial Strains, Plasmids, Enzymes, and Chemicals. *Escherichia coli* strain BL21(DE3) (Invitrogen) was used to express lipase constructs. Plasmids and their sources are as follows: pEML37, H. K. Kim;[22] pHOPE, J. S. Rhee;[23] pSLE2, T. K. Oh;[24] and pET26b, Novagen. Genotech synthesized the oligonucleotides used in this work (Table S2). All enzymes were purchased from New England BioLabs, except *Taq* polymerase (TaKaRa Bio Inc.). All antibiotics were purchased from Sigma-Aldrich. Ampicillin and kanamycin were used at final concentrations of 50 and 25 μg/mL, respectively. All *p*-nitrophenolate esters and triglyceride substrates [*p*-nitrophenyl caprate (*p*NPC), *p*-nitrophenyl laurate (*p*NPL)] as well as analytical standards (palmitic acid methyl ester, stearic acid methyl ester, oleic acid methyl ester, linoleic acid methyl ester, and linolenic acid methyl ester), olive oil, and palm oil were purchased from Sigma-Aldrich. Methanol was purchased from Merck Chemical Co. All recombinant DNA techniques were performed according to those described by Sambrook and Russel.[41]

Construction of a Gene Encoding a Lipase Fused to an Amphipathic Peptide (AP) and a Coiled-Coil Peptide (CCP). To increase the accessibility of hydrophobic substrates to a lipase, the APs BR2, BR3, and NKC (Figure S1) were fused to the N-terminus of lipase M37 (GenBank Acc. No. AY527197)[22] from *Photobacterium lipolyticum*, lipase L1 (GenBank Acc. No. U78785)[23] from *Geobacillus stearothermophilus*, and lipase TliA (GenBank Acc. No. AF083061)[24] from *Pseudomonas fluorescens*. These manipulations were performed using DNA sequences encoding AP-fused lipases M37, L1, or TliA that were PCR-amplified from pEML37, pHOPE, and pSLE2, respectively, using a forward primer representing the respective AP sequence and the 5′ sequence of each lipase and a reverse primer corresponding to the 3′ sequence of each lipase (Table S2). Each amplicon was digested with NdeI and XhoI and inserted into the NdeI/XhoI sites of pET26b to generate pM37, pBR2-M37, pBR3-M37, pNKC-M37, pL1, pBR2-L1, pBR3-L1, pNKC-L1, pTliA, pBR2-TliA, pBR3-TliA, and pNKC-TliA.

To further increase the accessibility between the AP-fused lipase and its substrate, we designed oligomeric bundles of the AP-fused lipases with a short CCP conjugated to the C-terminus of each (Table S3). These manipulations were performed using PCR amplification of the DNA sequences encoding each short CCP, the dimeric coiled-coil domain of yeast GCN4,[25] the tetrameric domain of chicken matrilin1 (MAT),[21] and the pentameric domain of rat cartilage oligomeric matrix protein (COMP).[28] The primers specific for each CCP are described in Table S2, which includes the DNA sequence of each CCP and the two repeats of a flexible G_4S linker at the N-terminus of the CCP DNA. The PCR-

DOI: 10.1021/cs502079g
ACS Catal. 2015, 5, 5016−5025

amplified CCP fragments were then digested with XbaI and XhoI and cloned into the XbaI/XhoI sites of pNKC-M37, producing pNKC-M37-GCN4, pNKC-M37-MAT, and pNKC-M37-COMP. To reveal the effect of CCP alone, genes encoding M37 lipase and CCPs were annealed by recombinant PCR and cloned into the NdeI/XhoI site of pET26b to generate pM37-GCN4, pM37-MAT, and pM37-COMP. To confirm the oligomerization of the lipases, the monomeric and oligomeric lipases were subjected to gel filtration chromatography using a Superdex-200 10/300 GL column (Amersham Biosciences) equilibrated and eluted with potassium phosphate buffer (50 mM, pH 7.0) containing 150 mM NaCl. The lipases were applied to a glow-discharged carbon-coated 400 mesh copper grid (Electron Microscopy Science), which was negatively stained with 0.75% uranyl formate and observed using a transmission electron microscope (TEM). Images were collected using an FEI 4 K × 4 K Eagle HS CCD camera connected to an FEI Tecnai T120 microscope operated at 120 kV. The defocus and nominal magnification for all images were −1 μm and 67 000×, respectively.

Expression and Purification of the Engineered Lipases. *E. coli* BL21(DE3) was transformed with each expression vector (pM37, pBR2-M37, pBR3-M37, pNKC-M37, pL1, pBR2-L1, pBR3-L1, pNKC-L1, pTliA, pBR2-TliA, pBR3-TliA, pNKC-TliA, pNKC-M37-GCN4, pNKC-M37-MAT, and pNKC-M37-COMP), inoculated into 3 mL of LB medium supplemented with 50 μg/mL of ampicillin and cultured at 37 °C for 12 h. Each culture was then diluted 1:100 into fresh medium (100 mL), and grown at 18 °C with constant shaking at 220 rpm. When the optical density of the cultures measured at 600 nm reached 0.6, protein expression was induced by adding 0.1 mM isopropyl-β-D-thiogalactopyranoside. The cells were harvested 16 h after induction by centrifugation at 6 000 rpm for 10 min at 4 °C and were lysed using sonication (6 × 3 min, Vibra-Cell VC750, Sonics) in a buffer containing 50 mM Tris-HCl (pH 8.0) and 200 mM NaCl. The clear supernatants, obtained after centrifugation at 10 000 rpm for 15 min at 4 °C, were processed for protein purification using a Ni-nitrilotriacetic acid agarose affinity column. The affinity resin was equilibrated with 50 mM Tris-HCl (pH 8.0) buffer containing 200 mM NaCl, and the bound proteins were eluted with a step gradient of imidazole (50, 100, 250, and 350 mM) and dialyzed using the same buffer. The purified proteins were loaded onto a cation-exchange HiTrap SP column (GE Healthcare Life Sciences) and eluted with a 0 to 1 M NaCl gradient. Fractions containing recombinant lipase were further purified by gel-filtration chromatography on a Superdex 200 column (Amersham Biosciences) equilibrated with 50 mM Tris-Cl, pH 8.0, and 150 mM NaCl. The cellular protein content was estimated using the bicinchoninic acid protein assay (Pierce) and bovine serum albumin (0.05−2 mg/mL) as the standard.[41]

Measurement of Catalytic Activity of Engineered Lipases. The catalytic activities (U/mg) of the wild-type and engineered lipases were measured using a standard spectrophotometric method[42] to detect *p*-nitrophenol using *p*-nitrophenyl derivatives (*p*NPC and *p*NPL). The reaction mixture (1 mL) contained 10 μL of *p*NPL (10 mM in acetonitrile), 40 μL of ethanol, and 950 μL of Tris-HCl buffer (50 mM, pH 8.0). The enzyme (10 μg) was added to the reaction mixture and incubated for 3 min at 40 °C, and the amount of *p*-nitrophenol produced was measured at 405 nm. Enzyme activity (1 unit) was defined as the quantity of enzyme that generated 1 μmol *p*-nitrophenol/min. Lipase catalytic activity was also measured by titrating the free fatty acids released by hydrolysis of olive oil and palm oil, using the pH-STAT method.[42] An emulsion of 5 mL of olive oil in 495 mL of 20 mM NaCl, 1 mM $CaCl_2$, and 0.5% (w/v) gum arabic solution was prepared using a Waring blender set to maximum speed for 2 min. After adjusting the substrate emulsion (20 mL) to pH 8.0 with 10 mM NaOH, 10 μg of enzyme was added. Fatty acid production was measured for 5 min at 40 °C using a pH titrator (718 Stat Titrino, Metrohm). One unit of lipase activity was defined as the amount of enzyme that generated 1 μmol fatty acid/min. To measure the accessibility of a lipase for its substrate, the K_m value was calculated from kinetics of *p*NPL hydrolysis. The rates of hydrolysis of *p*NPL by the wild-type and engineered lipases were determined in 150 μL reaction volumes containing 10 μg of lipase at 40 °C using an integrated robotic Infinite 200 Pro microplate reader (Tecan). The production of *p*-nitrophenolate was measured at 405 nm. All experiments were repeated three times. Kinetic constants were calculated by fitting the initial rates to the Michaelis−Menten equation.[43]

Analysis of Lipase−Substrate Interactions Using Fluorescence Microscopy. To determine the effects of AP and CCP on the accessibility of a lipase to its substrate, fluorescence microscopy analysis was performed. The engineered lipases were labeled with fluorescein isothiocyanate (FITC) according to the manufacturer's instructions (Calbiochem). FITC-labeled lipases were dialyzed against 50 mM Tris-HCl (pH 8.0) and 200 mM NaCl to eliminate unlabeled FITC. Olive oil was dissolved in distilled water at a 1:9 ratio and vortexed for 3 min. FITC-labeled lipases were added to the oil solution, and the mixture was incubated at 37 °C for 30 min to reach an equilibrium of binding and release of oil and lipases.[44] After the reaction was terminated, the interaction between lipases and oil was imaged using a Leica DM4000 fluorescence microscope. Images were acquired using a 488 nm bandpass excitation filter.

Thermal Stability and Methanol Tolerance of Engineered Lipases. The thermal stabilities of the engineered lipases were determined by measuring activity after incubation for 30 min at temperatures ranging from 4 to 70 °C. The catalytic activities of each lipase were assayed using the *p*-nitrophenol method described above. To analyze the thermal denaturation of the lipases, circular dichroism (CD) experiments were performed using a J-815 spectropolarimeter (JASCO Corporation) equipped with a Peltier system to control sample temperature. Purified proteins were subjected to ultrafiltration (Amicon Ultra-4 centrifugal filter unit, Millipore) to exchange the buffer to 50 mM sodium phosphate (pH 8.0), and protein concentrations were adjusted to 1 mg/mL. Far-UV spectra were analyzed after incubating the enzyme solutions for 30 min at 20 °C. Thermal ramps were performed using increments of 10 °C from 20 to 70 °C, and spectra were acquired after 3 min at each temperature. CD spectra were acquired in the far-UV region (190−260 nm) employing a 1 mm path-length quartz cuvette, a data pitch of 0.1 nm, and a scan speed of 20 nm/min. Five spectra were acquired and averaged for each sample. Thermal denaturation was monitored by following ellipticity at 193, 208, and 222 nm to determine α-helical content at 10 °C/min heating rate from 20 to 70 °C. The methanol resistance of each engineered lipase was determined by measuring the residual activity after methanol treatment. The reaction mixture contained enzyme (final

DOI: 10.1021/cs502079g
ACS Catal. 2015, 5, 5016−5025

concentration, 10 μg/mL) with the three different concentrations (3.3%, 5%, and 10% v/v) of methanol to provide oil:methanol molar ratios ranging from 1:1 to 1:3. Tris-HCl buffer (50 mM, pH 8.0) was added to a final volume of 1 mL, the mixture was incubated at 40 °C for 12 h, and then the catalytic activity was determined at specified times using the standard *p*NPC-spectrophotometry method described above.

Biodiesel Production Using Engineered Lipases. Each of wild-type M37, NKC-M37, and tetrameric NKC-M37-MAT lipases (30 mg) was incubated with 7.89 mL of olive oil, palm oil, or waste oil in a 30 mL glass-capped tube and shaken at 220 rpm in a rotary shaker at 40 °C, where methanol at three different molar ratio was added stepwise (one-, two-, and three-step processes).

After adding the lipases, the conversion rates were measured for 48 h. In the three-step process (one molar equivalent of methanol), the lipases and 0.33 mL of methanol were added to the tube at 0, 9, and 18 h. In the two-step process (1.5-mol equiv of methanol), the lipases and 0.495 mL of methanol were added at 0 and 12 h. In the one-step process (3 mol equiv of methanol), the lipases and 0.99 mL of methanol were added at 0 h. Samples (200 μL) were taken from the reaction mixture at the specified times and mixed with 1 mL of hexane in a 1.5-ml airtight vial and mixed for 2 min. After centrifugation at 1000*g* for 10 min, 10 μL of the upper layer was applied to a silica-gel plate to measure the amount of biodiesel produced and subjected to thin-layer chromatography (TLC). Hexane/ethyl acetate/acetic acid (90:10:1) and methanol/sulfuric acid (1:1) were used as the developing solvent and color reagent, respectively. After development, the TLC plate was sprayed with the color reagent, heated at 250 °C, and analyzed using gas chromatography (GC) (Hewlett-Packard 5890 Series II). The biodiesel yield is expressed as the percentage of the theoretical yield (ME%). The fatty acid methyl ester was analyzed using an HP-5 column (cross-linked 5% PH ME Siloxane, 0.32 mm × 30 mm id) and a flame ionization detector. The column temperature was increased from 70 to 300 °C at 10 °C/min and maintained at 300 °C for 3 min. The total quantities (in moles) of biodiesel in the reaction mixtures were calculated by comparisons of the retention times and peak areas of standard fatty acid methyl ester peaks.

■ ASSOCIATED CONTENT

Supporting Information

The Supporting Information is available free of charge on the ACS Publications website at DOI: 10.1021/cs502079g.

Helical wheel projection, the effects of CCPs on the catalytic activity of the lipase, Michaelis−Menten kinetics, the effects of the AP and CCP on the thermal stability of lipase, biodiesel production, sequences of the primers, and oligonucleotides used to construct the CCP domains (PDF)

■ AUTHOR INFORMATION

Corresponding Authors

*E-mail: (S.C.K.) sunkim@kaist.ac.kr.

*E-mail: (H.M.K.)hm_kim@kaist.ac.kr.

Author Contributions

⊥These authors contributed equally to this work (K.S.Y. and B.H.S.).

Notes

The authors declare no competing financial interest.

■ ACKNOWLEDGMENTS

This work was supported in part by the Intelligent Synthetic Biology Center of the Global Frontier Project (2011-0031955) funded by the Ministry of Science, ICT and Future Planning, Republic of Korea; the KRIBB Research Initiative Program; and the Next-Generation BioGreen 21 Program (SSAC, grant number PJ008110) funded by the Rural Development Administration, Republic of Korea.

■ REFERENCES

(1) Houde, A.; Kademi, A.; Leblanc, D. *Appl. Biochem. Biotechnol.* **2004**, *118*, 155−170.

(2) Hasan, F.; Shah, A. A.; Hameed, A. *Enzyme Microb. Technol.* **2006**, *39*, 235−251.

(3) Jaeger, K. E.; Eggert, T. *Curr. Opin. Biotechnol.* **2002**, *13*, 390−397.

(4) Ghanem, A.; Aboul-Enein, H. Y. *Chirality* **2005**, *17*, 1−15.

(5) Jegannathan, K. R.; Abang, S.; Poncelet, D.; Chan, E. S.; Ravindra, P. *Crit. Rev. Biotechnol.* **2008**, *28*, 253−264.

(6) Akoh, C. C.; Chang, S. W.; Lee, G. C.; Shaw, J. F. *J. Agric. Food Chem.* **2007**, *55*, 8995−9005.

(7) Leung, D. Y. C.; Wu, X.; Leung, M. K. H. *Appl. Energy* **2010**, *87*, 1083−1095.

(8) Meher, L. C.; Sagar, D. V.; Naik, S. N. *Renewable Sustainable Energy Rev.* **2006**, *10*, 248−268.

(9) Hobden, R. *Inform* **2014**, *25*, 143−144.

(10) Goto, M.; Kameyama, H.; Goto, M.; Miyata, M.; Nakashio, F. *J. Chem. Eng. Jpn.* **1993**, *26*, 109−111.

(11) Klahn, M.; Lim, G. S.; Seduraman, A.; Wu, P. *Phys. Chem. Chem. Phys.* **2011**, *13*, 1649−1662.

(12) Glogauer, A.; Martini, V. P.; Faoro, H.; Couto, G. H.; Muller-Santos, M.; Monteiro, R. A.; Mitchell, D. A.; de Souza, E. M.; Pedrosa, F. O.; Krieger, N. *Microb. Cell Fact.* **2011**, *10*, 54.

(13) Kim, E. Y.; Oh, K. H.; Lee, M. H.; Kang, C. H.; Oh, T. K.; Yoon, J. H. *Appl. Environ. Microb* **2009**, *75*, 257−260.

(14) Eijsink, V. G. H.; Gaseidnes, S.; Borchert, T. V.; van den Burg, B. *Biomol. Eng.* **2005**, *22*, 21−30.

(15) Lehmann, M.; Wyss, M. *Curr. Opin. Biotechnol.* **2001**, *12*, 371−375.

(16) Svendsen, A. *Biochim. Biophys. Acta, Protein Struct. Mol. Enzymol.* **2000**, *1543*, 223−238.

(17) Arnold, F. H. *Nature* **2001**, *409*, 253−257.

(18) Singh, R. K.; Tiwari, M. K.; Singh, R.; Lee, J. K. *Int. J. Mol. Sci.* **2013**, *14*, 1232−1277.

(19) Godoy, C. A.; de las Rivas, B.; Filice, M.; Fernandez-Lorente, G.; Guisan, J. M.; Palomo, J. M. *Process Biochem.* **2010**, *45*, 534−541.

(20) Watanabe, Y.; Shimada, Y.; Sugihara, A.; Noda, H.; Fukuda, H.; Tominaga, Y. *J. Am. Oil Chem. Soc.* **2000**, *77*, 355−360.

(21) Dames, S. A.; Kammerer, R. A.; Wiltscheck, R.; Engel, J.; Alexandrescu, A. T. *Nat. Struct. Mol. Biol.* **1998**, *5*, 687−691.

(22) Yang, K. S.; Sohn, J. H.; Kim, H. K. *J. Biosci Bioeng* **2009**, *107*, 599−604.

(23) Eom, G. T.; Song, J. K.; Ahn, J. H.; Seo, Y. S.; Rhee, J. S. *Appl. Environ. Microbiol.* **2005**, *71*, 3468−3474.

(24) Kim, M. H.; Kim, H. K.; Lee, J. K.; Park, S. Y.; Oh, T. K. *Biosci., Biotechnol., Biochem.* **2000**, *64*, 280−286.

(25) O'Shea, E. K.; Klemm, J. D.; Kim, P. S.; Alber, T. *Science* **1991**, *254*, 539−544.

(26) Cho, C. H.; Kammerer, R. A.; Lee, H. J.; Steinmetz, M. O.; Ryu, Y. S.; Lee, S. H.; Yasunaga, K.; Kim, K. T.; Kim, I.; Choi, H. H.; Kim, W.; Kim, S. H.; Park, S. K.; Lee, G. M.; Koh, G. Y. *Proc. Natl. Acad. Sci. U. S. A.* **2004**, *101*, 5547−5552.

(27) Kim, H. Z.; Jung, K.; Kim, H. M.; Cheng, Y.; Koh, G. Y. *Biochim. Biophys. Acta, Mol. Cell Res.* **2009**, *1793*, 772−780.

(28) Malashkevich, V. N.; Kammerer, R. A.; Efimov, V. P.; Schulthess, T.; Engel, J. *Science* **1996**, *274*, 761−765.

DOI: 10.1021/cs502079g
ACS Catal. 2015, 5, 5016−5025

(29) Goutelle, S.; Maurin, M.; Rougier, F.; Barbaut, X.; Bourguignon, L.; Ducher, M.; Maire, P. *Fundam. Clin. Pharmacol.* **2008**, *22*, 633−648.
(30) Kelly, S. M.; Price, N. C. *Curr. Protein Pept. Sci.* **2000**, *1*, 349−384.
(31) Shimada, Y.; Watanabe, Y.; Samukawa, T.; Sugihara, A.; Noda, H.; Fukuda, H.; Tominaga, Y. *J. Am. Oil Chem. Soc.* **1999**, *76*, 789−793.
(32) Brzozowski, A. M.; Derewenda, U.; Derewenda, Z. S.; Dodson, G. G.; Lawson, D. M.; Turkenburg, J. P.; Bjorkling, F.; Huge-Jensen, B.; Patkar, S. A.; Thim, L. *Nature* **1991**, *351*, 491−494.
(33) Romero, O.; Rivero, C. W.; Guisan, J. M.; Palomo, J. M. *PeerJ* **2013**, *1*, e27.
(34) Romero, O.; Filice, M.; de las Rivas, B.; Carrasco-Lopez, C.; Klett, J.; Morreale, A.; Hermoso, J. A.; Guisan, J. M.; Abian, O.; Palomo, J. M. *Chem. Commun. (Cambridge, U. K.)* **2012**, *48*, 9053−9055.
(35) Jung, S. K.; Jeong, D. G.; Lee, M. S.; Lee, J. K.; Kim, H. K.; Ryu, S. E.; Park, B. C.; Kim, J. H.; Kim, S. J. *Proteins: Struct., Funct., Genet.* **2008**, *71*, 476−484.
(36) Buchner, A.; Tostevin, F.; Hinzpeter, F.; Gerland, U. *J. Chem. Phys.* **2013**, *139*, 135101.
(37) Couture, M.; Yeh, S. R.; Wittenberg, B. A.; Wittenberg, J. B.; Ouellet, Y.; Rousseau, D. L.; Guertin, M. *Proc. Natl. Acad. Sci. U. S. A.* **1999**, *96*, 11223−11228.
(38) Qian, Z.; Fields, C. J.; Lutz, S. *ChemBioChem* **2007**, *8*, 1989−1996.
(39) Straathof, A. J. J. *Biotechnol. Bioeng.* **2003**, *83*, 371−375.
(40) Behzadi, S.; Farid, M. M. *Asia-Pac. J. Chem. Eng.* **2007**, *2*, 480−486.
(41) Sambrook, J. F.; Russell, D. W. *Molecular cloning: A laboratory manual*, 3rd ed.; Cold Spring Harbor Laboratory Press: Cold Spring Harbor, NY, 2001.
(42) Beisson, F.; Tiss, A.; Riviere, C.; Verger, R. *Eur. J. Lipid Sci. Technol.* **2000**, *102*, 133−153.
(43) Deichmann, U.; Schuster, S.; Mazat, J. P.; Cornish-Bowden, A. *FEBS J.* **2014**, *281*, 435−463.
(44) Ringsdorf, H. In *Physical Chemistry of Biological Interfaces*; Baszkin, A., Norde, W., Eds.; Marcel Dekker, Inc.: New York, 2000; pp 243−282.

DOI: 10.1021/cs502079g
ACS Catal. 2015, 5, 5016−5025